AIMS Mathematics, 7(4): 6128–6152.
DOI: 10.3934/math.2022341
Received: 02 December 2021
Revised: 06 January 2022
Accepted: 11 January 2022
Published: 17 January 2022

http://www.aimspress.com/journal/Math

Research article

Thermal vibration in rotating nanobeams with temperature-dependent due to exposure to laser irradiation

Ahmed E. Abouelregal[1,2,*], Khalil M. Khalil[1], Wael W. Mohammed[3,5] and Doaa Atta[4,5]

[1] Department of Mathematics, College of Science and Arts, Al-Qurayat, Jouf University, Saudi Arabia
[2] Basic Sciences Research Unit, Jouf University
[3] Department of Mathematics, Faculty of Science, University of Ha'il, Ha'il 2440, Saudi Arabia
[4] Department of Mathematics, College of Science, Qassim University, P.O. Box 6644, Buraydah 51482, Saudi Arabia
[5] Department of Mathematics, Faculty of Science, Mansoura University, Mansoura 35516, Egypt

* **Correspondence:** Email: ahabogal@ju.edu.sa; Tel: +966531095740.

Abstract: Effective classical representations of heterogeneous systems fail to have an effect on the overall response of components on the spatial scale of heterogeneity. This effect may be critical if the effective continuum subjects' scale differs from the material's microstructure scale and then leads to size-dependent effects and other deviations from conventional theories. This paper is concerned with the thermoelastic behavior of rotating nanoscale beams subjected to thermal loading under mechanical thermal loads based on the non-local strain gradient theory (NSGT). Also, a new mathematical model and governing equations were constructed within the framework of the extended thermoelastic theory with phase delay (DPL) and the Euler-Bernoulli beam theory. In contrast to many problems, it was taken into account that the thermal conductivity and specific heat of the material are variable and linearly dependent on temperature change. A specific operator has been entered to convert the nonlinear heat equation into a linear one. Using the Laplace transform method, the considered problem is solved and the expressions of the studied field variables are obtained. The numerical findings demonstrate that a variety of variables, such as temperature change, Coriolis force due to rotation, angular velocity, material properties, and nonlocal length scale parameters, have a significant influence on the mechanical and thermal waves.

Keywords: Rotating nanobeams; thermoelasticity; nonlocal strain gradient theory; variable properties; DPL model

Mathematics Subject Classification: 74A35, 80A19, 74F05, 65M60

1. Introduction

Nanotechnology is an expanding topic of research with numerous fields, for example, nanomedicine, nanofabrication, nanoelectronics, and nanomachines. These areas require novel devices, such as nano water harvesters, oscillators, load sensors, nano-scale mass sensors, field-emitting devices, biological tissues, and nano-electrical devices. Although the movement of nuclear energy and the forces working between them is usually successful, engineers rely on continuous theories that describe the influence of those phenomena in a far wider and intermediate sense in the case of the deformation of solids [1]. Even current digital computers need too much processing capacity to be used by the designer in comprehensive atomic simulations of engineering structures and components; the fundamental reason for these approximation theories is efficiency [2]. Continuous theories such as linear elasticity, plasticity, etc. give approximately a fraction of the cost of a simple nuclear simulation to approximate response engineers.

Several bulk material theories, such as the local beam, shell, and plate, were used in classical continuum mechanics to study the mechanical nanostructure of large-scale systems. While many studies have been done using classical continuum mechanics, its use at the nanoscale is unclear. Because in conventional continuum mechanics, small-scale factors such as Van der Waals, surface influences, lattice distance, energy, and chemical bonds are ignored [3].

Experimental as well as atomic simulation results show that these small-scale effects cannot be ignored at the nanoscale [4]. As the lattice distance between the atoms becomes increasingly relevant on a small scale, the discrete structure (interior) of the material cannot be homogenized into a continuum anymore. Nonlocal continuum theories have been defined to treat small-scale effects. In continuum modeling, this incorporates a size-dependent parameter to reflect the modest effect [5]. The theory of strain gradient, stress theory, the theory of micropolar, and the nonlocal theory of elasticity are among the most popular non-local theories [6, 7].

Eringen's nonlocal elasticity theory is effective in dealing with phenomena that have fewer origins in systems than in traditional models of communication [8–10]. The internal size or scale in this theory may be described simply as material parameters in the constitutive equations. These nonlocal mechanics are widely recognized and used for many issues, including wavy diffusion, dislocation, problems with cracks, etc. It has recently been shown that the application of non-local continuum mechanics to the modeling and analysis of nanostructures is very interesting [11]. Furthermore, few studies have reached the same conclusions as the classical theory of nonlocal elasticity [12].

Lim et al. [13] introduced the higher-order nonlocal strain gradient theory (NSGT) with two separate small-scale parameters in order to solve these problems with the nonlocal theory of elasticity. According to the NSGT, stress is the function of strain and a larger order strain gradient at every point in the domain. This theory takes into account both the interatomic forces and the deformation process of the higher-order microstructure. Subsequently, many studies using the NSGT theory have been carried out to examine the mechanical interaction of nanostructures [14]. The wave dispersion achieved by the NSGT theory is found to be extremely close to what was predicted by the dynamic molecular modeling of the nanopillars [15]. Liu et al. [16] evaluated the significant nanowire deformation behavior in terms of its surface influences (surface elasticity and residual surface stress). They

constructed the governing equation in combination with the residual surface stress and surface elasticity of nanowires with large displacements and different boundary conditions. Many researchers in many different applications [16–25] have used these modified models. The study of the dynamic behavior of rotating nanobeams is a growing research topic, due to its potential for application in various rotating NEMS such as nanomotors, nanoturbines, rotating nanomotors, etc. [26–41].

Generalized thermoelasticity theories have been developed to solve the infinite speed heat propagation problems predicted by the classical thermoelastic theory. By substituting a unique law of thermal conductivity for the standard Fourier law, Lord and Shulman [42] proposed one of the modified generalized thermoelasticity theories with one relaxation time. Recently, the Tzou model is one of the most recent models that has gained fame in the field of thermoelasticity [43–45]. In order to address the problems of the infinite speed of thermal waves, which are anticipated by conventional thermoelastic theory, several proposals have been offered in addition to the above-mentioned models [46–49].

Many studies focusing on the dynamics, bending, statics, and vibrational properties of nanobeams have been presented, with few studies focusing on the thermal elastic behavior of small-sized rotating beams with variable physical properties. In this paper, motivated by the need for improvement, the dynamic transverse vibration properties and thermal vibration analyzes of rotating nanobeams are studied based on the proposal of a new methodology based on nonlocal strain gradient theory (NSGT) that captures the small-scale effects. Also, the equations for the governing system were derived based on the Euler-Bernoulli theory and generalized thermoelasticity with two-phase lag (DPL). Contrary to many other concerns, the thermal conductivity and specific heat of the material have been considered variable and linearly dependent on changes in temperature.

The proposed model is able to study rotating nanobeams under thermal loads and includes Coriolis effects caused by rotation. To the authors' knowledge, for the first time, a rotational model of a thermal nanobeam has been reported whose properties depend on the temperature change. This study will also contribute to a full understanding of the behavior of rotating nanobeams, which have variable physical properties. The Laplace transform method was used to solve constitutive equations and partial differential governing equations, and is an important addition to this article. The Laplace transforms are inverted using a numerical approach based on Fourier series expansions. According to the numerical results, the mechanical and thermal wave responses of the rotating nanobeam are greatly influenced by many parameters such as temperature change, angular velocity, nonlocality parameters, and thermal conductivity change. The results of this study may be useful for future research and accurate design of nanomachines, such as nanoparticle bearings and nanogears, etc.

2. Theoretical preliminaries and basic equations

2.1. The nonlocal elasticity theory

According to the nonlocal elasticity theory of Eringen [8–10], the nonlocal stress-tensor τ_{ij} can be expressed as

$$\tau_{ij}(\boldsymbol{x}) = \int_V K_1(|\boldsymbol{x}, \boldsymbol{x}'|, \xi_1)\, \sigma_{ij}(\boldsymbol{x}')\mathrm{d}V(\boldsymbol{x}'), \tag{1}$$

where $\sigma_{ij}(\boldsymbol{x}')$ is the classical local stress tensor given by

$$\sigma_{ij}(\boldsymbol{x}') = 2\mu\varepsilon_{ij}(\boldsymbol{x}') + \big(\lambda\varepsilon_{kk}(\boldsymbol{x}') - \gamma\theta(\boldsymbol{x}')\big)\delta_{ij}, \tag{2}$$

The strain tensor ε_{ij} at any two adjacent points $\boldsymbol{x}'$ and $\boldsymbol{x}$, is defined by

$$\varepsilon_{ij}(\boldsymbol{x}') = 0.5\left(\frac{\partial u_i(x\prime)}{\partial x_j'} + \frac{\partial u_j(x\prime)}{\partial x_i'}\right). \tag{3}$$

In these equations, $\gamma = \frac{\alpha_t E}{(1-2\nu)} = \alpha_T E$, ν Poisson's ratio, E Young's modulus, α_t linear thermal expansion, u_i displacement components, δ_{ij} is the Kronecker delta, $\theta = T - T_0$ temperature change, and T_0 environmental temperature. The Lamé constants λ and μ can be written as $\lambda = E\nu/(1+\nu)(1-2\nu)$ and $\mu = E/2(1+\nu)$. Also, $K_1(|\boldsymbol{x}, \boldsymbol{x}'|, \xi_1)$ scalar kernel function, $\|\boldsymbol{x} - \boldsymbol{x}'\|$ Euclidean distance, $\xi_1 = e_0 a/l$ nonlocal scale parameter, a internal characteristic length, l external characteristic length, and e_0 determined experimentally.
When the kernel K_1 is chosen as [50,51]:

$$K_1(|\boldsymbol{x}, \boldsymbol{x}'|, \xi_1) = \frac{1}{2\pi\xi_1^2 l^2} K_0\left(\frac{\|x-x'\|}{\xi_1 l}\right), \tag{4}$$

where K_0 is the modified Bessel function, Eq (1) is given by [8–10]:

$$(1 - \xi_1^2\nabla^2)\tau_{ij}(\boldsymbol{x}) = \sigma_{ij}(\boldsymbol{x}'). \tag{5}$$

Using Eq (4) in (1), the nonlocal constitutive is obtained as

$$(1 - (e_0 a)^2\nabla^2)\tau_{ij} = C_{ijkl}\varepsilon_{kl} - \gamma_{ij}\theta. \tag{6}$$

According to the NSGT, the total stress tensor $T_{ij}(\boldsymbol{x})$ can be expressed as [17,52]

$$T_{ij}(\boldsymbol{x}) = \tau_{ij}(\boldsymbol{x}') - \nabla^2\sigma_{ij}^{(1)}(\boldsymbol{x}'), \tag{7}$$

where $\sigma_{ij}^{(1)}$ is the higher-order stress tensor given by [52,53]

$$\sigma_{ij}^{(1)}(\boldsymbol{x}') = l_m^2 \int_V K_2(|\boldsymbol{x}, \boldsymbol{x}'|, \xi_2)\, \sigma_{ij}(\boldsymbol{x}')\mathrm{d}V(\boldsymbol{x}'), \tag{8}$$

The material length scale parameter l_m was introduced to describe the importance of the higher-order strain gradient stress field, the additional attenuation kernel $K_2(|\boldsymbol{x}, \boldsymbol{x}'|, \xi_2)$ was introduced to describe the nonlocal effect of the higher-order strain gradient field, $\xi_2 = e_1 a/l$, and e_1 the related material constant [13]. By assuming that the attenuation kernels satisfy the conditions of Eringen's nonlocal elasticity, the differential counterpart of Eq (4) is written as [13,52–55]:

$$(1 - \xi_2^2\nabla^2)(1 - \xi_1^2\nabla^2)\tau_{ij} = (1 - \xi_2^2\nabla^2)\sigma_{ij} - l_m^2(1 - \xi_1^2\nabla^2)\nabla^2\sigma_{ij}. \tag{9}$$

For simplicity, assuming that $\xi_2 = \xi_1 = \xi$, the first-order nonlocal strain gradient model (NSGT) is given by

$$(1-\xi^2\nabla^2)\tau_{ij} = (1-l_m^2\nabla^2)\sigma_{ij}. \tag{10}$$

By inserting Eq (2) into (10), then we have

$$(1-(e_0a)^2\nabla^2)\tau_{ij} = (1-l_m^2\nabla^2)\big(C_{ijkl}\varepsilon_{kl}-\gamma_{ij}\theta\big). \tag{11}$$

When $l_m = 0$, the constitutive equation for the nonlocal elasticity theory can be obtained. On the other hand, if we set $\xi^2 = (e_0a)^2 = 0$, we may get the constitutive equation for strain gradient theory.

A micro/nanoscale size influence, for example, is represented by a stiffer elastic response to external stresses. This has been found in the plastic deformation of metals and polymers. In terms of the size effect on elasticity, Lam et al. [54] discovered a rise in the bending rigidities of epoxy micro-beams. When the beam thicknesses were reduced from 120 to 20 μm, the bending rigidities were roughly 2.4 times higher than expected by conventional theory. Similarly, additional studies have revealed an apparent rise in Young's modulus without reference to higher-order models. In the absence of strain gradients (for instance, in uniaxial tensile testing), Lam et al. [54] demonstrated that the elastic response of epoxy is independent of sample thickness, which is supported by strain gradient theories.

2.2. The dual-phase-lag thermoelastic mode (DPL)

The classical Fourier's law and energy equation for a homogeneous, isotropic, thermoelastic are as follows:

$$\vec{q} = -K\,\vec{\nabla}\theta, \tag{12}$$

$$\rho C_E\frac{\partial\theta}{\partial t} + T_0\gamma\frac{\partial e}{\partial t} = -\vec{\nabla}.\vec{q} + Q. \tag{13}$$

Combining (1) and (2) yields the classical heat conduction equation as

$$\rho C_E\frac{\partial\theta}{\partial t} + \gamma T_0\frac{\partial e}{\partial t} - \rho Q = K\nabla^2\theta. \tag{14}$$

Tzou [43–45] devised the dual-phase-lag (DPL) model that ignores instantaneous temperature-energy interactions. The DPL model, in particular, makes heat transmission in thermoelastic materials accurate and easy. The modified Fourier law, which has been superseded by Tzou [43–45], can be expressed as

$$\left(1+\tau_q\frac{\partial}{\partial t}\right)\vec{q} = -K\left(1+\tau_\theta\frac{\partial}{\partial t}\right)\nabla\theta. \tag{15}$$

The proposed new generalized dual-phase-lag thermoelastic model can be obtained by combining (13) and (15) as

$$\left(1+\tau_\theta\frac{\partial}{\partial t}\right)\big(\nabla\cdot\nabla(K\theta)\big) = \left(1+\tau_q\frac{\partial}{\partial t}+\tfrac{1}{2}\tau_q^2\frac{\partial^2}{\partial t^2}\right)\left(\rho C_E\frac{\partial\theta}{\partial t}+\gamma T_0\frac{\partial e}{\partial t}-\rho Q\right). \tag{16}$$

In Eqs (12)–(16), $\vec{q}$ is the heat flux vector, Q is the heat source, K is the thermal conductivity,

C_E is the specific heat, ρ is the material density, $e = \operatorname{div}\vec{u}$, τ_q is the phase lag of heat flux, and τ_θ is the temperature gradient's phase lag. Equation (16) is simplified to the constitutive relation of the LS model by setting $\tau_\theta = 0$ and omitting the influence of the term τ_q^2. Equation (7) can be reduced to the classical Fourier law when $\tau_q = \tau_\theta = 0$.

3. Problem formulation

As shown in Figure 1, a nanobeam with length L, width b and thickness h, internal cross-sectional area A, and bending stiffness EI are the components of the system under discussion. Under the Euler-Bernoulli principle, every plane cross-section is perpendicular to the nanobeam pivot in the beginning and perpendicular to the unbiased surface. The displacements are given by [53]

$$u = -z\frac{\partial w}{\partial x}, \quad v = 0, \quad w = w(x,t), \tag{17}$$

where w is the deflection.

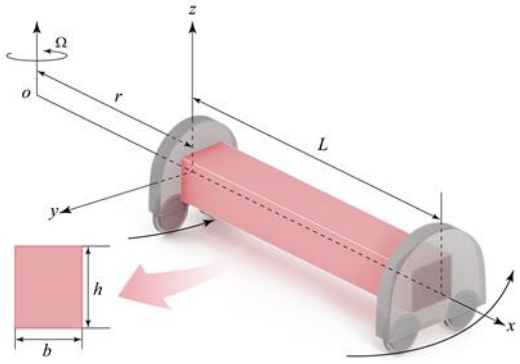

Figure 1. Schematic chart for the rotating nanobeam.

Equation (17) can be used to simplify Eq (9) as

$$\left(1 - \xi^2\frac{\partial^2}{\partial x^2}\right)\sigma_x = -E\left(1 - l_m^2\frac{\partial^2}{\partial x^2}\right)\left(z\frac{\partial^2 w}{\partial x^2} + \alpha_T\theta\right), \tag{18}$$

where σ_x is the nonlocal axial stress, $\alpha_T = \alpha_t/(1-2\nu)$ and $\xi = (e_0 a)^2$.

The bending moment $M(x,t)$ is given by:

$$M(x,t) = \int_{-h/2}^{h/2} z\sigma_x \mathrm{d}z. \tag{19}$$

Substituting Eq (18) into Eq (19), we get

$$\left(1 - \xi^2\frac{\partial^2}{\partial x^2}\right)M = -EI\left(1 - l_m^2\frac{\partial^2}{\partial x^2}\right)\left(\frac{\partial^2 w}{\partial x^2} + \alpha_T M_T\right), \tag{20}$$

where $I = bh^3/12$ and

$$M_T = \frac{12}{h^3}\int_{-h/2}^{h/2}\theta(x,z,t)z\mathrm{d}z. \tag{21}$$

The transverse motion equation can be written as [51]

$$\frac{\partial^2 M}{\partial x^2} = \rho bh\frac{\partial^2 w}{\partial t^2}. \tag{22}$$

We suppose that the nanobeam rotates about an axis parallel to the z-axis with an angular velocity Ω centered at a small distance r from the first edge of the nanobeam. The centrifugal tensional force $R(x)$ is introduced because of rotation. In this case, the equation of transverse motion (22) can be written as [27,28]

$$\frac{\partial^2 M}{\partial x^2} + \frac{\partial}{\partial x}\left(R(x)\frac{\partial w}{\partial x}\right) = \rho bh\frac{\partial^2 w}{\partial t^2}. \tag{23}$$

The axial force $R(x)$ due to centrifugal stiffening at a distance x from the origin (Figure 1) is given by [27,28,39]

$$R(x) = \int_x^L \rho A\Omega^2(r+x)dx. \tag{24}$$

After integration, Eq (24) can be simplified as

$$\begin{aligned} R(x) &= \frac{\rho A\Omega^2}{2}[(L+r)^2 - (L+x)^2] \\ &= \frac{\rho A\Omega^2}{2}[(r-x)(2L+r+x)]. \end{aligned} \tag{25}$$

By inserting (25) into Eqs (20) and (23), we can obtain

$$M(x,t) = \xi^2\left(\rho A\frac{\partial^2 w}{\partial t^2} - \frac{\partial}{\partial x}\left(R(x)\frac{\partial w}{\partial x}\right)\right) - EI\left(1 - l_m^2\frac{\partial^2}{\partial x^2}\right)\left(\frac{\partial^2 w}{\partial x^2} + \alpha_T M_T\right), \tag{26}$$

$$\begin{aligned} &\left[IE\left(l_m^2\frac{\partial^2}{\partial x^2} - 1\right)\frac{\partial^4}{\partial x^4} - \rho A\frac{\partial^2}{\partial t^2}\left(1 - \xi^2\frac{\partial^2}{\partial x^2}\right)\right]w + \left(1 - \xi^2\frac{\partial^2}{\partial x^2}\right)\left[\frac{\partial}{\partial x}\left(R(x)\frac{\partial w}{\partial x}\right)\right] \\ &\qquad -EI\alpha_T\left(1 - l_m^2\frac{\partial^2}{\partial x^2}\right)\frac{\partial^2 M_T}{\partial x^2} = 0. \end{aligned} \tag{27}$$

The modified heat conduction Eq (16) can be written as $(Q = 0)$

$$\left(1 + \tau_\theta\frac{\partial}{\partial t}\right)\nabla.(K\nabla\theta) = \left(1 + \tau_q\frac{\partial}{\partial t} + \frac{\tau_q^2}{2}\frac{\partial^2}{\partial t^2}\right)\frac{\partial}{\partial t}\left(\rho C_E\theta - \gamma T_0 z\frac{\partial^2 w}{\partial x^2}\right). \tag{28}$$

4. Thermal properties of materials

The conductivity K is considered a linear function of the temperature variation as [23,39,40]

$$K = K(\theta) = K_0(1 + K_1\theta), \tag{29}$$

where K_0 denotes the thermal conductivity at temperature T_0 and K_1 is the temperature-dependent thermal conductivity fluctuation.

By substituting Eq (29) into (28), we obtain

$$K_0\left(1+\tau_\theta\frac{\partial}{\partial t}\right)\nabla.\left((1+K_1\theta)\nabla\theta\right)=\left(1+\tau_q\frac{\partial}{\partial t}+\frac{\tau_q^2}{2}\frac{\partial^2}{\partial t^2}\right)\frac{\partial}{\partial t}\left(\rho C_E\theta-\gamma T_0 z\frac{\partial^2 w}{\partial x^2}\right). \quad (30)$$

To linearize the governing equation (30), we define a variable ψ as follows [39,40]

$$\psi=\int_0^\theta\frac{K(\theta)}{K_0}\mathrm{d}\theta \quad (31)$$

After inserting Eq (29) into Eq (31) and integrating, we have

$$\psi=\theta\left(1+\tfrac{1}{2}K_1\theta\right) \quad (32)$$

By differentiating the relationship (31) times in terms of distances and once in terms of time, we get

$$\begin{aligned}\nabla\psi&=\frac{K(\theta)}{K_0}\nabla\theta,\\ \frac{\partial\psi}{\partial t}&=\frac{K(\theta)}{K_0}\frac{\partial\theta}{\partial t}.\end{aligned} \quad (33)$$

Then, the heat conduction equation can be expressed as

$$\left(1+\tau_\theta\frac{\partial}{\partial t}\right)\left(\frac{\partial^2}{\partial x^2}+\frac{\partial^2}{\partial z^2}\right)\psi=\left(1+\tau_q\frac{\partial}{\partial t}+\tfrac{1}{2}\tau_q^2\frac{\partial^2}{\partial t^2}\right)\frac{\partial}{\partial t}\left(\frac{\rho C_E}{K}\psi-\frac{\gamma T_0}{K}z\frac{\partial^2 w}{\partial x^2}\right), \quad (34)$$

5. Sinusoidal solution

To solve the problem, we take the temperature change solution as a sinusoidal function as

$$\{\psi,\theta\}(x,z,t)=\{\Psi,\Theta\}(x,t)\sin\left(\frac{\pi}{h}z\right) \quad (35)$$

Presenting Eq (35) in Eqs (26), (27) and (34) leads to

$$\begin{aligned}\left[IE\left(l_m^2\frac{\partial^2}{\partial x^2}-1\right)\frac{\partial^4}{\partial x^4}-\rho A\frac{\partial^2}{\partial t^2}\left(1-\xi^2\frac{\partial^2}{\partial x^2}\right)\right]w+\left(1-\xi^2\frac{\partial^2}{\partial x^2}\right)\left[\frac{\partial}{\partial x}\left(R(x)\frac{\partial w}{\partial x}\right)\right]\\ -\frac{24EI\alpha_T}{\pi^2 h}\left(1-l_m^2\frac{\partial^2}{\partial x^2}\right)\frac{\partial^2\Psi}{\partial x^2}=0,\end{aligned} \quad (36)$$

$$\left(1+\tau_\theta\frac{\partial}{\partial t}\right)\left(\frac{\partial^2}{\partial x^2}-\frac{\pi^2}{h^2}\right)\Psi=\left(1+\tau_q\frac{\partial}{\partial t}+\tfrac{1}{2}\tau_q^2\frac{\partial^2}{\partial t^2}\right)\frac{\partial}{\partial t}\left(\frac{\rho C_E}{K}\Psi-\frac{\gamma T_0\pi^2 h}{24K}\frac{\partial^2 w}{\partial x^2}\right), \quad (37)$$

$$M(x,t)=\xi^2\left(\rho A\frac{\partial^2 w}{\partial t^2}-\frac{\partial}{\partial x}\left(R(x)\frac{\partial w}{\partial x}\right)\right)-EI\left(1-l_m^2\frac{\partial^2}{\partial x^2}\right)\left(\frac{\partial^2 w}{\partial x^2}+\frac{24\alpha_T}{\pi^2 h}\Theta\right). \quad (38)$$

The following non-dimensional variables are provided for convenience

$$\{u', x', L', w', z', h', b', l_m', \xi'\} = \eta c\{u, x, L, w, z, h, b, l_m, \xi\}, \{\Theta', \Psi'\} = \frac{1}{T_0}\{\Theta, \Psi\},$$
$$\{t', \tau_q', \tau_\theta'\} = \eta c^2\{t, \tau_q, \tau_\theta\}, \quad M' = \frac{1}{\eta cEI}M, \ \ c^2 = \frac{E}{\rho}, \eta = \frac{\rho C_E}{K}. \tag{39}$$

We can get the following after introducing dimensionless quantities (39) into the Eqs (36)–(38) (primes are omitted)

$$\left[\left(l_m^2\frac{\partial^2}{\partial x^2} - 1\right)\frac{\partial^4}{\partial x^4} - \frac{12}{h^2}\frac{\partial^2}{\partial t^2}\left(1 - \xi^2\frac{\partial^2}{\partial x^2}\right)\right]w + \left(1 - \xi^2\frac{\partial^2}{\partial x^2}\right)\left[\frac{\partial}{\partial x}\left(R(x)\frac{\partial w}{\partial x}\right)\right] - \frac{24T_0\alpha_T}{\pi^2 h}\left(1 - l_m^2\frac{\partial^2}{\partial x^2}\right)\frac{\partial^2\Psi}{\partial x^2} = 0, \tag{40}$$

$$\left(1 + \tau_\theta\frac{\partial}{\partial t}\right)\left(\frac{\partial^2}{\partial x^2} - \frac{\pi^2}{h^2}\right)\Psi = \left(1 + \tau_q\frac{\partial}{\partial t} + \frac{1}{2}\tau_q^2\frac{\partial^2}{\partial t^2}\right)\frac{\partial}{\partial t}\left(\Psi - \frac{\gamma\pi^2 h}{24K_0\eta}\frac{\partial^2 w}{\partial x^2}\right), \tag{41}$$

$$M(x,t) = \frac{12\xi}{h^2}\frac{\partial^2 w}{\partial t^2} - \xi^2\left[\frac{\partial}{\partial x}\left(R(x)\frac{\partial w}{\partial x}\right)\right] - \left(1 - l_m^2\frac{\partial^2}{\partial x^2}\right)\left(\frac{\partial^2 w}{\partial x^2} + \frac{24T_0\alpha_T}{\pi^2 h}\Theta\right). \tag{42}$$

The maximum axial force $R(x)$ due to centrifugal stiffening at the root ($x = 0$) is given by [38,39]

$$R_{max} = \int_0^L \rho A\Omega^2(r + x)dx = \frac{1}{2}\rho A\Omega^2 L(2r + L) \tag{43}$$

The motion Eq (40) can therefore be described as

$$\left[\left(l_m^2\frac{\partial^2}{\partial x^2} - 1\right)\frac{\partial^4}{\partial x^4} - \frac{12}{h^2}\frac{\partial^2}{\partial t^2}\left(1 - \xi^2\frac{\partial^2}{\partial x^2}\right)\right]w + q + \frac{6L\Omega^2(2r+L)}{h^2}\left(1 - \xi^2\frac{\partial^2}{\partial x^2}\right)\frac{\partial^2 w}{\partial x^2} - \frac{24T_0\alpha_T}{\pi^2 h}\left(1 - l_m^2\frac{\partial^2}{\partial x^2}\right)\frac{\partial^2\Psi}{\partial x^2} = 0. \tag{44}$$

The bending moment $M(x,t)$ in Eq (42) can also be expressed as

$$M(x,t) = \frac{12\xi^2}{h^2}\frac{\partial^2 w}{\partial t^2} - \xi^2\left[q + \frac{6L\Omega^2(2r+L)}{h^2}\frac{\partial^2 w}{\partial x^2}\right] - \left(1 - l_m^2\frac{\partial^2}{\partial x^2}\right)\left(\frac{\partial^2 w}{\partial x^2} + \frac{24T_0\alpha_T}{\pi^2 h}\Theta\right) \tag{45}$$

6. Laplace transform strategy

Using the Laplace technique under the initial conditions

$$\Psi(x,0) = 0 = \frac{\partial\Psi(x,0)}{\partial t},$$
$$w(x,0) = 0 = \frac{\partial w(x,0)}{\partial t}. \tag{46}$$

Then, Eqs (41), (44) and (45) are converted as

$$\left[\frac{\mathrm{d}^6}{\mathrm{d}x^4} - A_7\frac{\mathrm{d}^4}{\mathrm{d}x^4} + A_8\frac{\mathrm{d}^2}{\mathrm{d}x^2} - A_9\right]\overline{w} = A_{10}\left(1 - l_m^2\frac{\mathrm{d}^2}{\mathrm{d}x^2}\right)\frac{\mathrm{d}^2\overline{\Psi}}{\mathrm{d}x^2},$$
$$A_5\frac{\mathrm{d}^2\overline{w}}{\mathrm{d}x^2} = -\left(\frac{\mathrm{d}^2}{\mathrm{d}x^2} - A_6\right)\overline{\Psi}, \tag{47}$$

$$M(x,t) = l_m^2\left(\frac{\mathrm{d}^4}{\mathrm{d}x^4} - A_7\frac{\mathrm{d}^2}{\mathrm{d}x^2} + A_9\xi\right)\overline{w} - A_2\left(1 - l_m^2\frac{\mathrm{d}^2}{\mathrm{d}x^2}\right)\overline{\Theta}, \tag{48}$$

where

$$A_1 = \frac{6L\Omega^2(2r+L)}{h^2}, A_2 = \frac{24T_0\alpha_T}{\pi^2 h}, A_3 = \frac{\gamma\pi^2 h}{24K\eta}, A_4 = \frac{s\left(1+\tau_q s+s^2\tau_q^2/2\right)}{(1+\tau_\theta s)},$$
$$A_5 = A_3A_4,\ A_6 = \frac{\pi^2}{h^2} + A_4,\ A_0 = \frac{12s^2}{h^2}, A_7 = \frac{1+A_1\xi^2}{l_m^2}, \tag{49}$$
$$A_8 = \frac{A_1+A_0\xi^2}{l_m^2}, A_9 = \frac{A_0}{l_m^2},\ A_{10} = \frac{A_2}{l_m^2}.$$

We obtain from Eqs (47) and (48) the following

$$\left[\frac{\mathrm{d}^8}{\mathrm{d}x^8} - A\frac{\mathrm{d}^6}{\mathrm{d}x^6} + B\frac{\mathrm{d}^4}{\mathrm{d}x^4} - C\frac{\mathrm{d}^2}{\mathrm{d}x^2} + F\right]\bar{w} = 0, \tag{50}$$

where

$$A = A_7 + A_6, B = A_8 + A_7A_6 - l_m^2A_5A_{10},\ C = A_9 + A_8A_6 - A_5A_{10}, F = A_9A_6 \tag{51}$$

Equation (50) has a general solution that can be written as

$$\bar{w}(x,s) = \sum_{j=1}^{4}\left(C_j\mathrm{e}^{-m_jx} + C_{j+3}\mathrm{e}^{m_jx}\right), \tag{52}$$

where the parameters $C_j, (j = 1,2..,8)$ are the integrated parameters. Also, the parameters m_1^2, m_2^2, m_3^2 and m_4^2 satisfy the equation

$$m^8 - Am^6 + Bm^4 - Cm^2 + F = 0. \tag{53}$$

With the help of Eqs (48) and (52), we have

$$\bar{\Psi}(x,s) = \sum_{j=1}^{4} H_j\left(C_j\mathrm{e}^{-m_jx} + C_{j+3}\mathrm{e}^{m_jx}\right), \tag{54}$$

where $H_j = -\frac{A_5m_j^2}{m_j^2-A_6}$.

The axial displacement $\bar{u}$ is given by

$$\bar{u} = -z\frac{\mathrm{d}\bar{w}}{\mathrm{d}x} = z\sum_{j=1}^{4} m_j\left(C_j\mathrm{e}^{-m_jx} - C_{j+3}\mathrm{e}^{m_jx}\right). \tag{55}$$

After using the Laplace transform to Eq (35), the temperature $\bar{\theta}$ may be calculated as

$$\bar{\theta}(x,s) = \sin\left(\frac{\pi}{h}z\right)\left[\frac{-1+\sqrt{1+2K_1\bar{\psi}}}{K_1}\right]. \tag{56}$$

The bending moment $\bar{M}$ can be obtained from (48) after using the solutions (52) and (54).

7. Application

We assume that the nanobeam fulfills the following boundary conditions:

i) Mechanical boundary conditions [55]

$$w(x,t)|_{x=0,L} = 0,\quad \left.\frac{\partial^2 w(x,t)}{\partial x^2}\right|_{x=0,L} = 0,\quad \left.\frac{\partial^4 w(x,t)}{\partial x^4}\right|_{x=0,L} = 0. \tag{57}$$

ii) Thermal boundary conditions:

$$\Theta(x,t)|_{x=0} = \frac{L_0 t e^{(-t/t_p)}}{t_p^2} = L(t), \tag{58}$$

$$\frac{\partial \Theta(x,t)}{\partial x}\Big|_{x=L} = 0 \tag{59}$$

In Eq (58), t_p is the time length of a laser pulse and L_0 the laser intensity. Introducing Eqs (32) and (33) into Eqs (58) and (59), we get

$$\Psi(0,t) = L(t) + \tfrac{1}{2} K_1 [L(t)]^2, \tag{60}$$

$$\frac{\partial \Psi(L,t)}{\partial x} = 0. \tag{61}$$

In the Laplace transform domain, the boundary conditions (57)–(61) can be written as

$$\bar{w}(x,s)|_{x=0,L} = 0, \ \frac{\mathrm{d}^2 \bar{w}(x,s)}{\mathrm{d}x^2}\Big|_{x=0,L}, \ \frac{\mathrm{d}^4 \bar{w}(x,s)}{\mathrm{d}x^4}\Big|_{x=0,L} = 0, \tag{62}$$

$$\bar{\Psi}(x,s)|_{x=0} = \frac{L_0}{(1+st_p)^2} + \frac{K_1 L_0^2}{t_p(2+st_p)^3} = \bar{G}(s), \tag{63}$$

$$\frac{\mathrm{d}\bar{\Psi}}{\mathrm{d}x}\Big|_{x=L} = 0. \tag{64}$$

When the previously mentioned conditions are applied, then we have

$$\sum_{j=1}^{4} \left(C_j + C_{j+3}\right) = 0, \tag{65}$$

$$\sum_{j=1}^{4} \left(C_j \mathrm{e}^{-m_j L} + C_{j+3} \mathrm{e}^{m_j L}\right) = 0, \tag{66}$$

$$\sum_{j=1}^{4} m_j^2 \left(C_j + C_{j+3}\right) = 0, \tag{67}$$

$$\sum_{j=1}^{4} m_j^2 \left(C_j e^{-m_j L} + C_{j+3} e^{m_j L}\right) = 0, \tag{68}$$

$$\sum_{j=1}^{4} m_j^4 \left(C_j + C_{j+3}\right) = 0, \tag{69}$$

$$\sum_{j=1}^{4} m_j^4 \left(C_j e^{-m_j L} + C_{j+3} e^{m_j L}\right) = 0, \tag{70}$$

$$\sum_{j=1}^{4} H_j \left(C_j + C_{j+3}\right) = \bar{G}(s), \tag{71}$$

$$\sum_{j=1}^{4} m_j H_j \left(C_j e^{-m_j L} - C_{j+3} e^{m_j L}\right) = 0. \tag{72}$$

By solving the aforementioned system equations, the unknown parameters $C_j, (j = 1,2..,8)$ may be computed.

8. Laplace transform inversion

The Fourier series expansion, as well as the Honig and Hirdes technique [56], will be briefly introduced in this paper. In this method, all functions $\bar{g}(x,s)$ in the Laplace field can be converted to the time field $\bar{g}(x,s)$ by using the following relation:

$$g(x,t) = \frac{2e^{ct}}{t_1}\left\{\frac{1}{2}\mathrm{Re}[\bar{g}(x,c)] + \mathrm{Re}\left[\sum_{n=1}^{N}\bar{g}\left(x, c+\frac{\mathrm{i}n\pi}{t_1}\right)\cos\left(\frac{n\pi t}{t_1}\right)\right]\right\}, \tag{73}$$

where the parameter t_1 denotes the time interval and Re stands for the real part of the complex function. By summing a specific number of N, Equation (80) can now be calculated numerically. As a result, c and N must be adjusted to improve accuracy [57,58].

9. Results and discussion

In this work, numerical results are provided by focusing on physical parameters and constants in SI units, which are used in formulating the physical variables under study, and by using silicon as a material. The following physical values are used [39]:

$$E = 169\ \mathrm{GPa},\ t_p = 2\ \mathrm{ps},\ \rho = 2330\frac{\mathrm{kg}}{\mathrm{m}^3}, L_0 = 1\times 10^{11}\frac{\mathrm{J}}{\mathrm{m}^2}\quad C_E = 713\frac{\mathrm{J}}{\mathrm{kg\,K}},\ K = 156\frac{\mathrm{W}}{\mathrm{mK}},$$
$$L/h = 5\,, b/h = 0.5, L = 1, z = h/3, \alpha_T = 2.59\times 10^{-9}\frac{1}{\mathrm{K}},\ \ \nu = 0.22, T_0 = 293\ K, t = 0.1.$$

We divided graphical representations of several properties, such as size-dependent effects (ξ and l_m), parameter change of thermal conductivity K_1, and rotation Ω on the investigated thermal-physical fields, into three groups in order to analyze their effects.

The current work was prompted by a strong fit between the conclusions of nonlocal strain gradient theory and evidence from experimental research and molecular dynamics simulations. The investigation of wave propagation in the classical theory was established using the NSG theory and the DPL heat transfer theory, and the calculation results were compared with the theoretical and experimental results [59,60]. The nonlocal strain gradient elasticity model, unlike the conventional model, can demonstrate good agreement with experimental results.

9.1. Effect of nonlocal and material length scale coefficients

Nonlocal gradient theory (NSGT) has been used to capture the size-dependent effect of the nanobeam, as well as other specific cases such as classical theory (CET), nonlocal theory (NET), and strain regression theory (SGT). A stress-gradient parameter ξ is also included to account for the stress gradient effect, as well as a strain-gradient parameter l_m to account for the strain gradient effect. If $l_m = 0$, the introduced nonlocal gradient theory (NSGT) model may be reduced to a nonlocal elastic model (NET), and if $\xi = 0$, to a strain gradient model (SGT).

Figures 2–5 show the dimensionless studied fields for various nonlocal parameter (ξ) and material length scale parameter (l_m) values. For the purposes of computing, the values $K_1 = -0.3,\ \Omega = 0.3,$

$\tau_q = 0.02$ and $\tau_\theta = 0.01$ are taken. The NSGT incorporates the impacts of both nonlocal and material length scale factors, allowing for a better understanding of the implications of these two parameters on the dynamic responses of the nanobeam. From the numerical results and figures, the following can be noted:

• It is clear that the non-local parameter and the stress gradient modulus have a great influence on the interactions within the nanobeam.

• The dimensionless values of deflection w and displacement u grow in proportion to the nonlocal parameter values. From Figures 2 and 4, it is apparent that the magnitudes of NSGT, SGT and NET models for deflections w and displacement u have greater values than those achieved using conventional continuum theory (CET).

• When the parameter $l_m > \xi$, the NSGT model yields lower results than the nonlocal elastic model (NET). These facts suggest the nanobeam has a stiffness-reduction impact when the length scale parameter is lower than the non-local parameter, and when the parameter of the material length scale is higher than the non-local parameter, the nanobeam exerts a stiffness-reduction effect. Thus, it can be said that the non-local parameter has the effect of stiffness-softening while the gradient modulus has the effect of stiffness-hardening. Similar results were also found in several papers, such as in [60–62] on the dynamic response of beam-type structures based on NSGT.

• From the figures, it is clear that the difference between the NSGT and SGT models is less pronounced at lower non-local parameter values but becomes more pronounced at larger non-local parameter values. This pattern applies to both the CET and the NET. Indeed, regarding the reduction of the results due to the raising of the non-local parameter values, one can mention that the strain increases while stress is reduced in Eringen's differential formulation. This phenomenon causes a softening of the effect. Thus, an increase in the non-local parameter decreases the aberrations within the nanobeam. Compared with the published results, the collected results show good agreement, for example, with those of Jena et al. [22] and Zeng et al. [23].

• Also, when the parameter l_m is smaller than the parameter ξ; the nonlocal effect predominates, which leads to a stiffness-softening effect of the nanobeam. When the parameter ξ is greater than the parameter l_m, the effect of the stress gradient takes precedence, causing the nanobeam to stiffen.

Figure 2 shows that the deflection w starts and terminates at zero values and fulfills the boundary conditions at $x = 0$ and $x = L$. It is further shown that the aberrations recorded by the Euler-Bernoulli beam theory are usually slower than those predicted by non-local beam theories, indicating that the nanobeam is attenuated and softened when the size-dependent is taken into account.

• From Figure 3, we notice that the parameters ξ and l_m have a very weak influence on the distribution of temperature change θ. Thermal waves are continuous and smooth phenomena that reach a steady state depending on the phase lag factors, which means that heat transfers easily from one particle to another, causing the temperature to drop even more. This phenomenon is in contrast to the traditional theory of thermal elasticity, which predicts that the rate of propagation of thermal perturbation is infinite.

• Increases in temperature and thermal load cause a drop in beam stiffness, which reduces thermal and mechanical waves.

• As seen in Figure 4 it is evident that the magnitude of the displacement u in the NSGT, SGT and NET models is less than that obtained using standard contact theory (CET).

• In contrast to the behavior shown in Figures 2 and 3, the bending moment M behavior as shown in Figures 5. It is clear that the sizes of the NSGT, SGT, and NET models of the bending moment M

have lower values than those achieved using the conventional contact theory (CET). In other words, the bending moment decreases with the height of the nonlocal modulus.

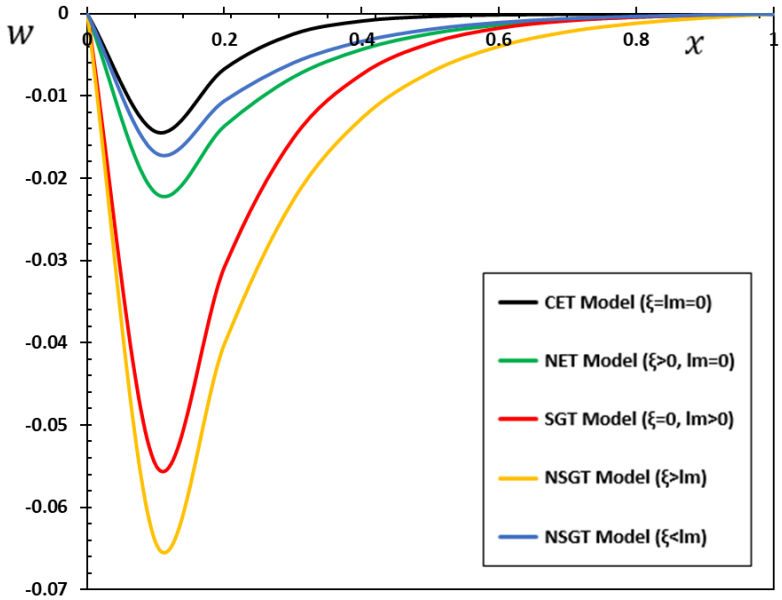

Figure 2. The deflection w via local and nonlocal models.

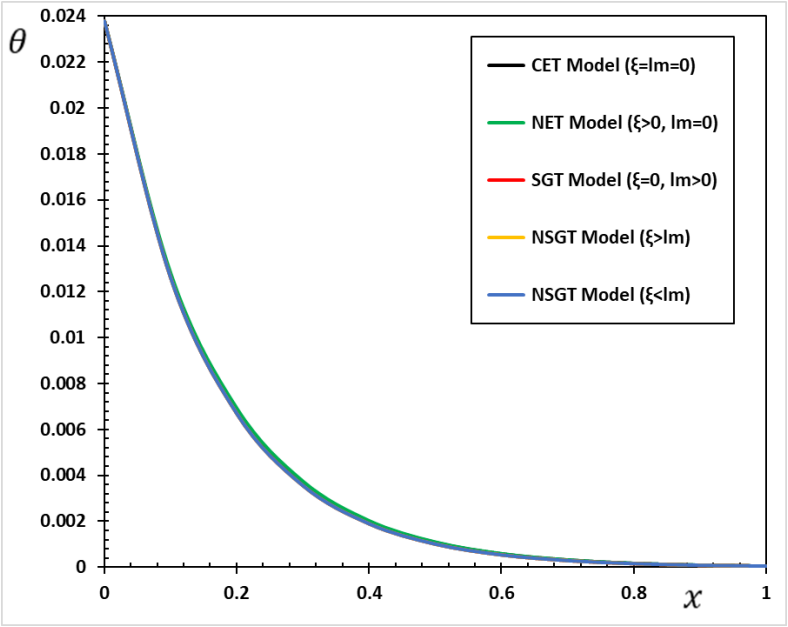

Figure 3. The temperature θ via local and nonlocal models.

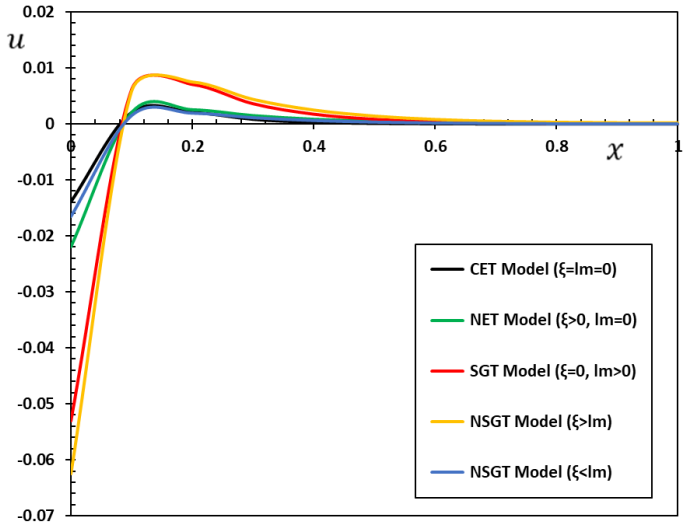

Figure 4. The displacement u via local and nonlocal models.

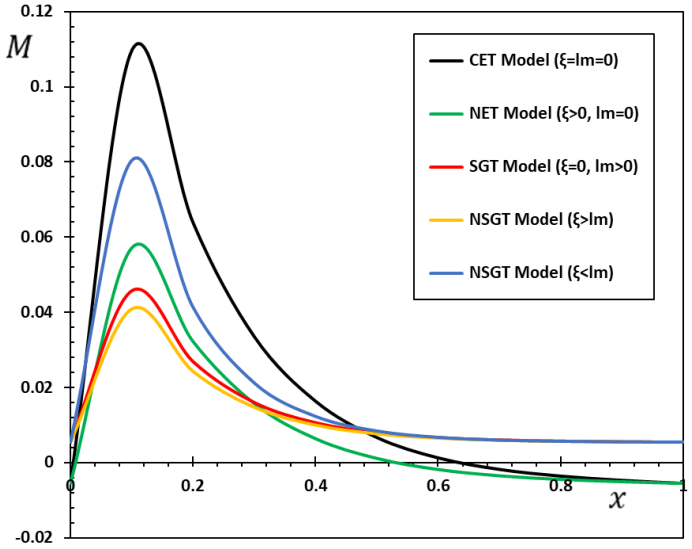

Figure 5. The bending moment M via local and nonlocal models.

• Finally, the classical theory, which does not take into account the size dependence and can yield results suitable for studying narrow beams, is well known. However, in non-local models, the effect of size-dependent mechanical behavior becomes significant and cannot be ignored. From theoretical calculations, we may conclude that the nanobeam can display either a hardening softening or a hardening-stiffness effect, depending on the relative amplitude of the non-local factor and the length-scale factor of the material.

• This may explain why the stiffness-hardening effect of nanobeams is frequently found in experimental studies as in [61], but the stiffness-softening effect of nanostructures is more common as discussed in [62].

9.2. The effect of the variability of thermal conductivity

Thermal conductivity is an important property of a material that is often taken for granted. On the other hand, many experimental and theoretical investigations have shown that thermal conductivity is closely related to temperature change [63,64]. Depending on the general one-dimensional thermoplastics problem, Xiong and Guo [65] emphasized the effect of changing temperature-dependent properties on field variables. As described earlier, the thermal conductivity K is assumed to be a linear function of the temperature change (see Eq (25)). A material with a high K is considered an excellent conductor of heat, while a material with a low K is considered a good thermal insulator. As a result, this parameter has a significant impact on both the working conditions in deep mines and the ability of subterranean vents to store thermal energy. It is also related to geothermal energy generation and radioactive waste disposal.

In this subsection, the effect of the variability parameter of thermal conductivity K_1 on the non-dimensional deflection, temperature spread, displacement, and bending moment is investigated. When the coefficient of thermal conductivity is dependent on heat, there will be two separate examples to study the change of thermal conductivity. The values $K_1 = -1$ and $K_1 = -0.5$ are used when the thermal conductivity is dependent on the temperature change. The value $K_1 = 0.0$ is utilized if the thermal conductivity is constant. The non-dimensional values $\xi = 0.01$, $l_m = 0.01$, $\Omega = 0.3$, $\tau_q = 0.02$ and $\tau_\theta = 0.01$ are taken. The numerical results of the studied field variables are depicted in Figures 6–9.

As can be seen from Figure 6, the magnitudes of w decrease as the parameter K_1 increases. As illustrated in Figure 7, as the distance x increases, the temperature drops, driving wave propagation. The temperature distribution is increased when the parameter K_1 is reduced. Physically, increasing the parameter K_1 improves the heat transfer process and raises the local temperature of the beam. It is also noted that with an increase in the parameter K_1, the temperature rises. The results were compared with those presented in [66] and it was found that there was agreement in the results.

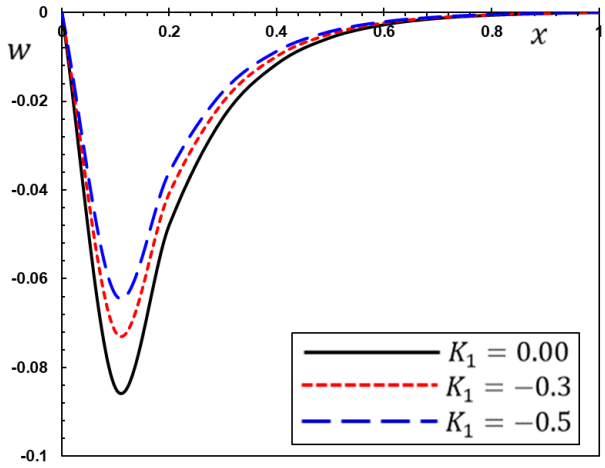

Figure 6. The deflection w versus x for different values of the parameter K_1.

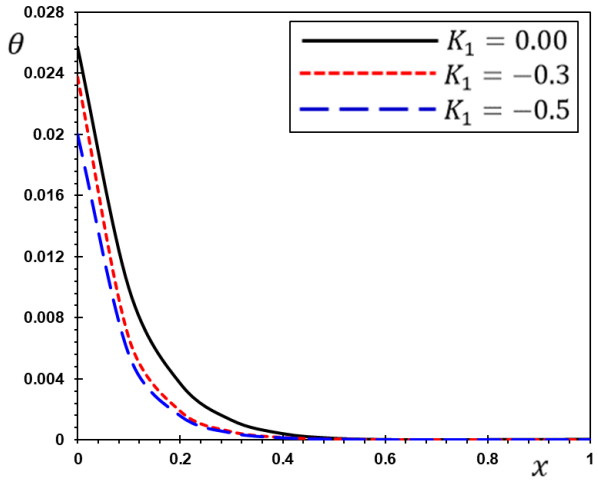

Figure 7. Temperature θ versus x for different values of the parameter K_1.

Figure 8 shows that the displacement u increases when $0.0 \leq x \leq 0.1$ for the greatest amplification and drops when $0.1 \leq x \leq 0.6$. In the last range $0.6 \leq x \leq 1$ of wave propagation, the displacement u is traveling straight. The variability parameter K_1 has a significant impact on the displacement. In Figure 9, the increase in the parameter K_1 is designed to enhance the distribution of the bending moment M.

The results demonstrate that the change in thermal conductivity has an effect that should not be ignored [67]. The mechanical and thermal distributions of the nanobeam reveal that the wave propagates as a velocity-limited wave in the medium and depends on the coefficient of change of thermal conductivity K_1 [34]. We may deduce from the analysis that the thermoelastic behavior is affected by variations in thermal material characteristics, and these impacts are mostly focused on the distribution's peak values.

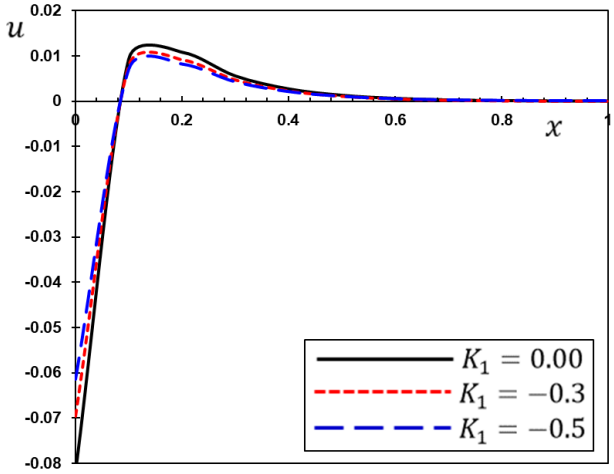

Figure 8. Displacement u versus x for different values of the parameter K_1.

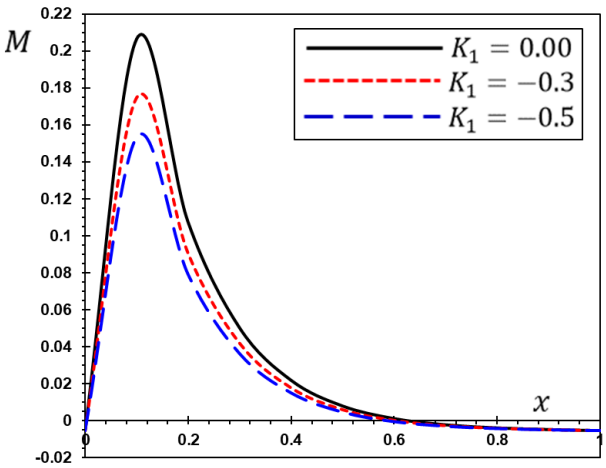

Figure 9. Bending moment M versus x for different values of the parameter K_1.

9.3. Effects of the rotation speed

As mentioned earlier, spinning nanobeams play an important role in many nano-devices, and properly modeling and studying them is a very challenging task. In this section, a study was conducted to investigate the effect of rotational speed Ω on the functions of the physical fields. Numerical calculations were performed when the values of the other effective parameters were constant. This work will use non-local gradient theory (NSGT) to elucidate the vibrational behavior of nanobeams for size-dependent beams, as there has been no precise inquiry into the nanobeams' rotation. It is found that the speed of rotation, elastic media, and non-local scaling factors greatly influence the bending vibration of the system.

Figures 10, 11, 12, and 13 show the variance of the investigated fields for three distinct angular velocity values ($\Omega = 0, 0.1, 0.3$). The rotation coefficient is zero ($\Omega = 0$) in the absence of rotation, which is a special case of the current work. Figure 10 depicts the rotation Ω that affects the deflection w. In the presence and absence of rotation (centrifugal force), this parameter was shown to have a significant impact on the deflection w and variance in results. It is noticeable that increasing the angular velocity Ω reduces the deflection w of the non-local transverse nanobeam. These findings and behavior are similar to those seen in [68,69]. In Figure 11, the effect of angular velocity on temperature change θ is examined and displayed. We note from the figure that the effect of rotation on the temperature change is very slight. The results of the preceding literature are compatible with those of the author, such as the equivalent results achieved in [37–39].

The effect of the angular velocity of rotation Ω on the variance of the displacement u is shown in Figure 12. It is found that the speed of rotation Ω most prominently affects the curves reflecting the displacement field. The figure also displays that the displacement distribution u decreases in certain periods with increasing rotation and rises in other periods along the axis of the beam. Figure 13 shows the changes in bending moment M for different values of rotational velocity Ω. The graph indicates that rotation greatly affects the moment curves and that as the angular velocity Ω values decrease, the bending moment amplitude M increases. Ultimately, the amplitude of the studied fields changes as the non-dimensional angular velocity increases. In other words, the speed of rotation Ω is most prominently responsible for the stiffening effect of the centrifugal force. The functional features

of rotating structures with diverging effects of external stimulation can be improved based on understanding the influence of rotational speed in hybrid nano-generators to achieve better shaft motion.

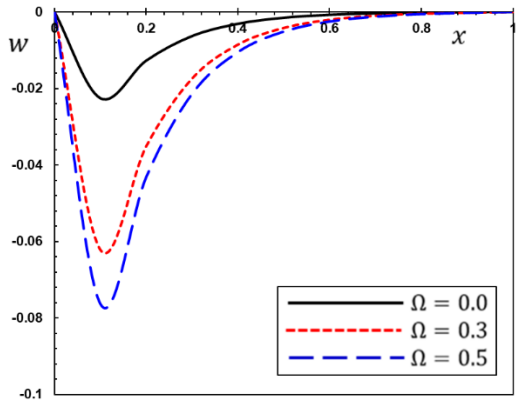

Figure 10. The deflection w with different rotational speed Ω.

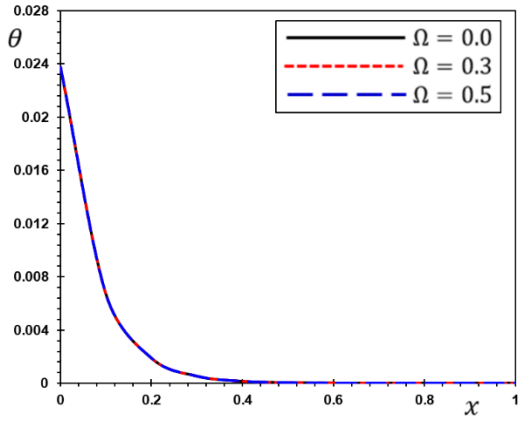

Figure 11. The temperature θ with different rotational speed Ω.

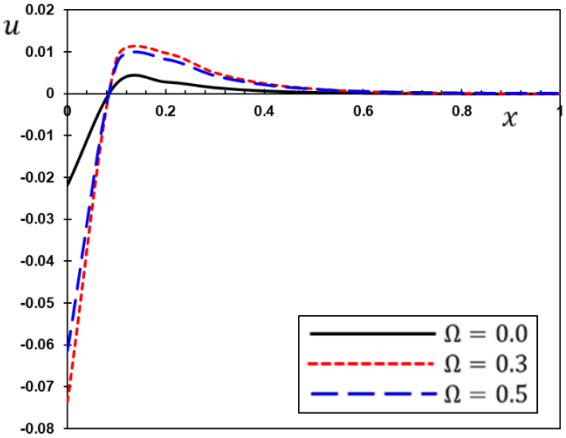

Figure 12. The displacement u with different rotational speed Ω.

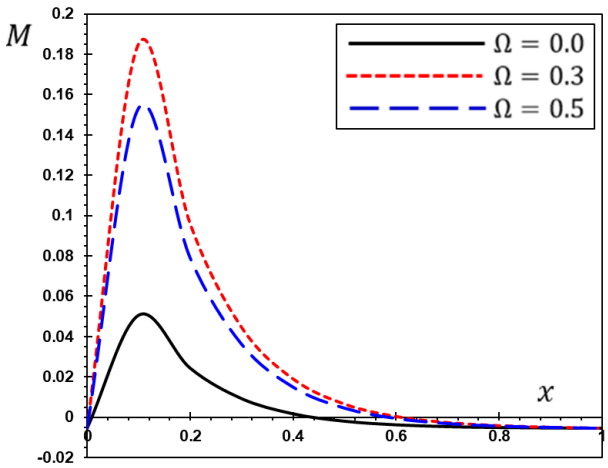

Figure 13. The bending moment M with different rotational speed Ω.

10. Conclusions

In the current work, a nonlocal strain gradient beam model is constructed to examine the vibration response of the thermoelastic nanobeam, including its rotational effect. The Euler–Bernoulli beam theory coupled with the generalized thermoelastic model with phase delays and nonlocal strain-gradient theory, is used to construct the governing equations for the rotating nanobeam. It was taken into consideration that the thermal conductivity coefficient and the specific heat of the nanobeam are temperature dependent. The effect of nonlocal, material length scale parameters, rotation, and thermal conductivity variability on thermal and mechanical wave scattering is investigated. The following important outcomes are achieved:

• The non-local gradient elasticity model showed results that were different from the results of the traditional model, and this is in agreement with the previous literature.

• Deflections and displacement are reduced as the non-local parameters increase. The strain gradient effect is a priority when the non-local parameter is greater than the length scale parameter of the material, which results in the annealing of the nanobeam.

• The difference between NSGT and SGT is less pronounced at lower non-local parameter values, but becomes more pronounced at larger non-local parameter values. This pattern applies to both the CET and the NET.

• The behavior of different fields is affected by changes in the thermal properties of materials, and these effects appear mostly in the peak values of the distributions.

• Depending on the relative amplitude of the nonlocal factor and the material length-scale parameter, the nanobeam may show the effect of stiffness-softening or stiffness-hardening.

• The fluctuation of thermal conductivity and its dependence on temperature change have a significant impact on different physical fields.

• The angular velocity of rotation is most prominently responsible for the strengthening effect of the centrifugal force.

• The effect of rotation on the temperature change is very slight. The fundamental effect of rotation on the behavior of different physical distributions can also be inferred from the obtained results and should be taken into account in production and design procedures.

• Temperature-dependent and size-dependent structures may both be found in nanoscale materials. This indicates that external temperature has a significant impact on nonlocality behavior. The rotating nanobeam can also respond as a temperature-dependent structure.

• Our findings reveal that the dependent size impact on the thermoelastic vibration of nanobeams could be significant, emphasizing the relevance of dependent size effects in nanoscale device and system design.

Conflict of interest

The authors declared no potential conflicts of interest with respect to the research.

Acknowledgments

The authors extend their appreciation to the Deanship of Scientific Research at Jouf University for funding this work through research grant No. (DSR2020-05-426). We would also like to extend our sincere thanks to the College of Science and Arts in Al-Qurayyat for its technical support.

References

1. V. S. Chandel, Gl. Wang, M. Talha, Advances in modelling and analysis of nano structures: A review, *Nanotechn. Rev*., **9** (2020), 230–258. https://doi.org/10.1515/ntrev-2020-0020
2. R. H. J. Peerlings, N. A. Fleck, Computational evaluation of strain gradient elasticity constants, *Int. J. Multiscale Comput. Eng*., **2** (2004), 599–619. https://doi.org/10.1615/IntJMultCompEng.v2.i4.60
3. B. I. Yakobson, C. Brabec, J. Bernholc, Nanomechanics of carbon tubes: Instabilities beyond linear response, *Phys. Rev. Lett.*, **76** (1996), 2511. https://doi.org/10.1103/PhysRevLett.76.2511
4. L. Behera, S. Chakraverty, Recent researches on nonlocal elasticity theory in the vibration of carbon nanotubes using beam models, *Arch. Comput. Meth. Eng*., **24** (2017), 481–494. https://doi.org/10.1007/s11831-016-9179-y
5. B. Arash, Q. Wang, A review on the application of nonlocal elastic models in modeling of carbon nanotubes and graphenes, *Comput. Mater. Sci*., **51** (2012), 303–313. https://doi.org/10.1016/j.commatsci.2011.07.040
6. Y. Liu, J. Reddy, A nonlocal curved beam model based on a modified couple stress theory, *Int. J. Struc. Stab. Dynam*., **11** (2011), 495–512. https://doi.org/10.1142/s0219455411004233
7. S. Park, X. Gao, Bernoulli-Euler beam model based on a modified couple stress theory, *J. Microm. Microeng*., **16** (2006), 2355. https://doi.org/10.1061/40830(188)166
8. A. C. Eringen, On differential equations of nonlocal elasticity and solutions of screw dislocation and surface waves, *J. Appl. Phys*., **54** (1983). 4703–4710. http://dx.doi.org/10.1063/1.332803
9. A. C. Eringen, *Nonlocal continuum field theories*. Springer Science & Business Media, Springer-Verlag: New York, 2002.
10. A. C. Eringen, D. Edelen, On nonlocal elasticity, *Int. J. Eng Sci*., **10** (1972), 233–248. https://doi.org/10.1016/0020-7225(72)90039-0
11. A. C. Eringen, *Nonlocal polar field theory*. In: A.C. Eringen (ed.), Continuum Physics. 4. Academic Press: New York, 1976.

12. A. Farajpour, M. H. Ghayesh, H. Farokhi, A review on the mechanics of nanostructures, *Int. J. Eng. Sci*., **133** (2018), 231–263. https://doi.org/10.1016/j.ijengsci.2018.09.006
13. C. Lim, G. Zhang, J. Reddy, A higher-order nonlocal elasticity and strain gradient theory and its applications in wave propagation, *J. Mech. Phys. Solids*, **78** (2015), 298–313. https://doi.org/10.1016/j.jmps.2015.02.001
14. E. C. Aifantis, On the role of gradients in the localization of deformation and fracture, *Int. J. Eng. Sci.*, **30** (1992), 1279–1299. https://doi.org/10.1016/0020-7225(92)90141-3
15. L. Li, Y. Hu, L. Ling, Wave propagation in viscoelastic single-walled carbon nanotubes with surface effect under magnetic field based on nonlocal strain gradient theory, *Physica E: Low-dimensional Sys. Nanostruc*., **75** (2016), 118–124. https://doi.org/10.1016/j.physe.2015.09.028
16. J. L. Liu, Y. Mei, R. Xia, W. L. Zhu, Large displacement of a static bending nanowire with surface effects, *Physica E: Low-Dimensional Sys. Nanostruc*., **44** (2012), 2050–2055. https://doi.org/10.1016/j.physe.2012.06.009
17. F. Yang, A. C. M. Chong, D. C. C. Lam, P. Tong, Couple stress based strain gradient theory for elasticity, *Int. J. Solids Struct.*, **39** (2002), 2731–2743. https://doi.org/10.1016/S0020-7683(02)00152-X
18. R. D. Mindlin, Second gradient of strain and surface-tension in linear elasticity, *Int. J. Solids Struct.*, **1** (1965), 417–438. https://doi.org/10.1016/0020-7683(65)90006-5
19. B. Akgöz, Ö. Civalek, A size-dependent shear deformation beam model based on the strain gradient elasticity theory, *Int. J. Eng. Sci.*, **70** (2013), 1–14. https://doi.org/10.1016/j.ijengsci.2013.04.004
20. R. Barretta, F. M. de Sciarra, Variational nonlocal gradient elasticity for nano-beams, *Int. J. Eng. Sci.*, **143** (2019), 73–91. https://doi.org/10.1016/j.ijengsci.2019.06.016
21. C. Li, H. Qing, C. F. Gao, Theoretical analysis for static bending of Euler–Bernoulli using different nonlocal gradient models, *Mech. Adv. Mater. Struct*., **28** (2020), 1965–1977. https://doi.org/10.1080/15376494.2020.1716121
22. S. K. Jena, S. Chakraverty, M. Malikan, H. Mohammad-Sedighi, Hygro-magnetic vibration of the single-walled carbon nanotube with nonlinear temperature distribution based on a modified beam theory and nonlocal strain gradient model, *Int. J. Appl. Mech*., **12** (2020), 2050054. https://doi.org/10.1142/S1758825120500544
23. S. Zeng, K. Wang, B. Wang, J. Wu, Vibration analysis of piezoelectric sandwich nanobeam with flexoelectricity based on nonlocal strain gradient theory, *Appl. Math. Mech.*, **41** (2020), 859–880. https://doi.org/10.1007/s10483-020-2620-8
24. P. Bian, H. Qing, On bending consistency of Timoshenko beam using differential and integral nonlocal strain gradient models, *ZAMM J. Appl. Math. Mech*., **101** (2021), e202000132. https://doi.org/10.1002/zamm.202000132
25. P. Jiang, H. Qing, C. Gao, Theoretical analysis on elastic buckling of nanobeams based on stress-driven nonlocal integral model, *Appl. Math. Mech.*, **41** (2019), 207–232. https://doi.org/10.1007/s10483-020-2569-6
26. P. Zhang, H. Qing, The consistency of the nonlocal strain gradient integral model in size-dependent bending analysis of beam structures, *Int. J. Mech. Sci.*, **189** (2021), 105991. https://doi.org/10.1016/j.ijmecsci.2020.105991
27. S. Narendar, S. Gopalakrishnan, Nonlocal wave propagation in rotating nanotube, *Results Phys.*, **1** (2011), 17–25. https://doi.org/10.1016/j.rinp.2011.06.002

28. F. Ebrahimi, M. R. Barati, P. Haghi, Wave propagation analysis of size-dependent rotating inhomogeneous nanobeams based on nonlocal elasticity theory, *J. Vibr. Control*, **24** (2018), 3809–3818. https://doi.org/10.1177/1077546317711537
29. M. Malik, D. Das, Free vibration analysis of rotating nano-beams for flap-wise, chord-wise and axial modes based on Eringen's nonlocal theory, *Int. J. Mech. Sci.*, **179** (2020), 105655. https://doi.org/10.1016/j.ijmecsci.2020.105655
30. L. Hao-nan, L. Cheng, S. Ji-ping, Y. Lin-quan, Vibration analysis of rotating functionally graded piezoelectric nanobeams based on the nonlocal elasticity theory, *J. Vibr. Eng. Techn.*, (2021), https://doi.org/10.1007/s42417-021-00288-9.
31. M. Mohammadi, M. Safarabadi, A. Rastgoo, A. Farajpour, Hygro-mechanical vibration analysis of a rotating viscoelastic nanobeam embedded in a visco-Pasternak elastic medium and in a nonlinear thermal environment, *Acta Mechanica*, **227** (2016), 2207–2232. https://doi.org/10.1007/s00707-016-1623-4
32. S. Faroughi, A. Rahmani, M. I. Friswell, On wave propagation in two-dimensional functionally graded porous rotating nano-beams using a general nonlocal higher-order beam model, *Appl. Math. Model.*, **80** (2020), 169–190. https://doi.org/10.1016/j.apm.2019.11.040
33. F. Ebrahimi, A. Dabbagh, Wave dispersion characteristics of rotating heterogeneous magneto-electro-elastic nanobeams based on nonlocal strain gradient elasticity theory, *J. Electro. Waves Applic.*, **32** (2018), 138–169. https://doi.org/10.1080/09205071.2017.1369903
34. A. Rahmani, B. Safaei, Z. Qin, On wave propagation of rotating viscoelastic nanobeams with temperature effects by using modified couple stress-based nonlocal Eringen's theory, *Eng. Comput.*, (2021). https://doi.org/10.1007/s00366-021-01429-0.
35. S. M. Ragab, A. E. Abouelregal, H. F. AlShaibi, R. A. Mansouri, Heat transfer in biological spherical tissues during hyperthermia of magnetoma, *Biology*, **10** (2021), 1259. https://doi.org/10.3390/biology10121259
36. A. Babaei, M. Arabghahestani, Free vibration analysis of rotating beams based on the modified couple stress theory and coupled displacement field, *Appl. Mech.*, **2** (2021), 226–238. https://doi.org/10.3390/applmech2020014
37. A. E. Abouelregal, H. Ahmad, Thermodynamic modeling of viscoelastic thin rotating microbeam based on non-Fourier heat conduction, *Appl. Math. Modell.*, **91** (2021), 973–988. https://doi.org/10.1016/j.apm.2020.10.006
38. A. E. Abouelregal, H. Ahmad, K. A. Gepreeld, P. Thounthong, Modelling of vibrations of rotating nanoscale beams surrounded by a magnetic field and subjected to a harmonic thermal field using a state-space approach, *Europ. Phys. J. Plus*, **136** (2021), 268. https://doi.org/10.1140/epjp/s13360-021-01257-7
39. A. E. Abouelregal, H. Ahmad, T. A. Nofal, H. Abu-Zinadah, Thermo-viscoelastic fractional model of rotating nanobeams with variable thermal conductivity due to mechanical and thermal loads, *Mod. Phys. Lett. B*, **35** (2021), 2150297. https://doi.org/10.1142/S0217984921502973
40. A. E. Abouelregal, H. M. Sedighi, S. A. Faghidian, A. H. Shirazi, Temperature-dependent physical characteristics of the rotating nonlocal nanobeams subject to a varying heat source and a dynamic load, *Facta Univer. Series: Mech. Eng.*, **19** (2021), 633–656. https://doi.org/10.22190/FUME201222024A

41. A. E. Abouelregal, H. M. Sedighi, The effect of variable properties and rotation in a visco-thermoelastic orthotropic annular cylinder under the Moore-Gibson-Thompson heat conduction model, *Proc. Institut. Mech. Eng., Part L: J. Mat.: Design Appl.*, **235** (2021), 1004–1020. https://doi.org/10.1177/1464420720985899
42. H.W. Lord, Y. H. Shulman, A generalized dynamical theory of thermoelasticity, *J. Mech. Phys. Solids*, **15** (1967), 299–309. https://doi.org/10.1016/0022-5096(67)90024-5
43. D. Y. Tzou, Thermal shock phenomena under high rate response in solids, *Annual Rev. Heat Trans.*, **4** (1992), 111–185. https://doi.org/10.1615/AnnualRevHeatTransfer.v4.50
44. D. Y. Tzou, A unified field approach for heat conduction from macro-to micro-scales, *J. Heat Trans.*, **117** (1995), 8–16. https://doi.org/10.1115/1.2822329
45. D. Y. Tzou, The generalized lagging response in small-scale and high-rate heating, *Int. J. Heat Mass Trans.*, **38** (1995), 3231–3240. https://doi.org/10.1016/0017-9310(95)00052-B
46. A. E. Abouelregal, Two-temperature thermoelastic model without energy dissipation including higher order time-derivatives and two phase-lags, *Mater. Res. Express*, **6** (2019), 116535. http://dx.doi.org/10.1088/2053-1591/ab447f
47. A. E. Abouelregal, On Green and Naghdi thermoelasticity model without energy dissipation with higher order time differential and phase-lags, *J. Appl. Comp. Mech.*, **6** (2020), 445–456. http://doi.org/10.22055/JACM.2019.29960.1649
48. A. E. Abouelregal, A novel generalized thermoelasticity with higher-order time-derivatives and three-phase lags, *Multidiscip. Model. Ma. Structures*, **16** (2020), 689–711. https://doi.org/10.1108/MMMS-07-2019-0138
49. A. E. Abouelregal, Three-phase-lag thermoelastic heat conduction model with higher-order time-fractional derivatives, *Indian J. Phys.*, **94** (2020), 1949–1963. https://doi.org/10.1007/s12648-019-01635-z
50. D. Singh, G. Kaur, S. K. Tomar, Waves in nonlocal elastic solid with voids, *J. Elast.*, **128** (2017), 85–114. https://doi.org/10.1016/j.euromechsol.2018.03.015
51. R. D. Mindlin, Micro-structure in linear elasticity, *Arch. Rat. Mech. Analy.*, **16** (1964), 51–78. https://doi.org/10.1007/BF00248490
52. M. Jirasek, Nonlocal theories in continuum mechanics, *Acta Polytech.*, **44** (2004), 16–34. https://doi.org/10.14311/610
53. J. Reddy, Nonlocal theories for bending, buckling and vibration of beams, *Int. J. Eng. Sci.*, **45** (2007), 288–307. https://doi.org/10.1016/j.ijengsci.2007.04.004
54. D. C. C. Lam, F. Yang, A. C. M. Chong, J. Wang, P. Tong, Experiments and theory in strain gradient elasticity, *J. Mech. Phys. Solids*, 51 (2003), 1477–1508. https://doi.org/10.1016/S0022-5096(03)00053-X
55. L. Li, H. Tang, Y. Hu, The effect of thickness on the mechanics of nanobeams, *Int. J. Eng. Sci.*, **123** (2018), 81–91. https://doi.org/10.1016/j.ijengsci.2017.11.021
56. G. Honig, U. Hirdes, A method for the numerical inversion of Laplace transform, *J. Comput. Appl. Math.*, **10** (1984), 113–132. https://doi.org/10.1016/0377-0427(84)90075-X
57. A. Cheng, P. Sidauruk, Approximate inversion of the Laplace transform, *Math. J.*, 4 (1994), 76–82. Corpus ID: 53626109
58. H. Hassanzadeh, M. Poolad-Darvish, Comparison of different numerical Laplace inversion methods for engineering application, *Appl. Math. Comput.*, **189** (2007), 1966–1981. https://doi.org/10.1016/j.amc.2006.12.072

59. B. Gu, T. He, Y. Ma, Thermoelastic damping analysis in micro-beam resonators considering nonlocal strain gradient based on dual-phase-lag model, *Int. J. Heat Mass Trans.*, **180** (2021), 121771. https://doi.org/10.1016/j.ijheatmasstransfer.2021.121771
60. X. Li, L. Li, Y. Hu, Z. Ding, W. Deng, Bending, buckling and vibration of axially functionally graded beams based on nonlocal strain gradient theory, *Comp. Struc.*, **165** (2017), 250–265. https://doi.org/10.1016/j.compstruct.2017.01.032
61. L. Lu, X. Guo, J. Zhao, A unified nonlocal strain gradient model for nanobeams and the importance of higher order terms, *Int. J. Eng. Sci.*, **119** (2017), 265–277. https://doi.org/10.1016/j.ijengsci.2017.06.024
62. L. Lu, X. Guo, J. Zhao, Size-dependent vibration analysis of nanobeams based on the nonlocal strain gradient theory, *Int. J. Eng. Sci.*, **116** (2017), 12–24. https://doi.org/10.1016/j.ijengsci.2017.03.006
63. X. Zhu, L. Li, Closed form solution for a nonlocal strain gradient rod in tension, *Int. J. Eng. Sci.*, **119** (2017), 16–28. https://doi.org/10.1016/j.ijengsci.2017.06.019
64. S. Singh, D. Kumar, K. N. Rai, Convective-radiative fin with temperature dependent thermal conductivity, heat transfer coefficient and wavelength dependent surface emissivity, *Propuls. Power Res.*, **3** (2014), 207–221. https://doi.org/10.1016/j.jppr.2014.11.003
65. C. B. Xiong, L. N. Yu, Y. B. Niu, Effect of variable thermal conductivity on the generalized thermoelasticity problems in a fiber-reinforced anisotropic half-space, *Advan. Mater. Sci. Eng.*, **2019** (2019), Article ID 8625371. https://doi.org/10.1155/2019/8625371
66. C. Xiong, Y. Guo, Effect of variable properties and moving heat source on magnetothermoelastic problem under fractional order thermoelasticity, *Advan. Mater. Sci. Eng.*, **2016** (2016), Article ID 5341569. https://doi.org/10.1155/2016/5341569
67. A. S. V. Kanth, N. U. Kumar, A haar wavelet study on convective-radiative fin under continuous motion with temperature-dependent thermal conductivity, *Walailak J. Sci. Techn.*, **11** (2014), 211–224. https://doi.org/10.14456/WJST.2014.40
68. Y. Wang, D. Liu, Q. Wang, J. Zhou, Asymptotic solutions for generalized thermoelasticity with variable thermal material properties, *Arch. Mech.*, **68** (2016), 181–202. https://doi.org/10.1142/S1758825113500233
69. F. Ebrahimi, P. Haghi, Elastic wave dispersion modelling within rotating functionally graded nanobeams in thermal environment, *Adv. Nano Res.*, **6** (2018), 201–217. https://doi.org/10.12989/anr.2018.6.3.201

AIMS Press